https://doi.org/10.3311/PPci.22007
Creative Commons Attribution

Periodica Polytechnica Civil Engineering, 67(3), pp. 775–784, 2023

Deterioration Effect of Sandstone Tensile Strength and Its Mesoscopic Mechanism under Dry-wet Cycles

Jianfei Yang[1], Guodong Zhang[1,2*], Lixu Deng[1,2], Yaxin Zhang[1], Zheng Li[1], Yicheng Ye[3]

[1] National Field Observation and Research Station of Landslides in Three Gorges Reservoir Area of Yangtze River, China Three Gorges University, 443002, Yichang, Hubei, China
[2] Key Laboratory of Geological Hazards on Three Gorges Reservoir Area, China Three Gorges University, Ministry of Education, 443002, Yichang, Hubei, China
[3] Hubei Hydrogeology and Engineering Geology Survey Institute, 443002, Yichang, Hubei, China
[*] Corresponding author, e-mail: zgd@ctgu.edu.cn

Received: 06 February 2023, Accepted: 31 March 2023, Published online: 12 April 2023

Abstract

The rock mass in the hydro-fluctuating zone of the reservoir bank slope is under dry-wet cycles for a long time, which will cause the deterioration of rock mass and induce geological disasters. In this study, a series of dry-wet cycle tests on the argillaceous quartz sandstone in the Three Gorges Reservoir area was carried out. Then, after different dry-wet cycles, the sandstone specimens were used to conduct the Brazilian splitting, scanning electron microscope, and 3D laser scanning tests. Herein, we provided detailed physical and microscopy image data to analyze the deterioration effect of tensile strength and mesostructure deterioration process of sandstone. With the increase of dry-wet cycles, the tensile strength of sandstone initially decreases rapidly, and then the decline rate tends to slow down. The evolution laws of fractal dimension and porosity are also significantly consistent with the deterioration of tensile strength. Moreover, further mesostructural analysis has revealed the repeated "absorption and swelling-dehydration and contraction" of clay minerals. This results in the breakage of framework mineral quartz and the expansion and connectivity of internal cracks, which ultimately deteriorates sandstone's tensile strength.

Keywords

tensile strength, mesostructure, dry-wet cycles, argillaceous quartz sandstone, rock deterioration

1 Introduction

Since the high water-level impoundment of the Three Gorges Reservoir area (TGRA) in 2008, the reservoir's water level has risen and fallen periodically between 145 m and 175 m above sea level annually. The formation of a 30 m hydro-fluctuation belt makes the rock mass in a state of dry-wet cycles all year round [1]. The water-rock interaction under this special condition inevitably leads to the deterioration of rock mass, which may have adverse effects on the stability of the bank slope. Yin et al. [2] have summarized numerous rock landslides in the TGRA, then concluded that such rock deterioration effect is one of the three major landslide-inducing factors. Therefore, it is of great theoretical and practical significance to study the deterioration effect of rock mass strength under dry-wet cycles to evaluate the evolution of bank slope stability.

As one of the most widely distributed lithologies in the TGRA, sandstone has been studied by various researchers on its macro-deterioration effect under dry-wet cycles [1]. With the increase of dry-wet cycles, the porosity, water absorption, and permeability of sandstone gradually increase, while the wave velocity of rock decreases [3–5]. It was also found through various mechanical tests that the mechanical parameters of sandstone deteriorated to varying degrees, such as compressive strength, tensile strength, shear strength, elastic modulus, cohesion, and internal friction angle [6–10]. As the tensile strength of sandstone materials is far below the compressive strength, the rock failure often starts with the tensile stress zone [11]. Therefore, it is very important to study the deterioration effect of sandstone tensile strength under dry-wet cycles. Liu et al. [11] selected a moderately weathered sandstone from the TGRA to conduct a series dry-wet cycle tests and found that the tensile strength decreased exponentially, and the damage degree of sandstone with thickness of

Cite this article as: Yang, J., Zhang, G., Deng, L., Zhang, Y., Li, Z. Ye, Y. "Deterioration Effect of Sandstone Tensile Strength and Its Mesoscopic Mechanism under Dry-wet Cycles", Periodica Polytechnica Civil Engineering, 67(3), pp. 775–784, 2023. https://doi.org/10.3311/PPci.22007

50 mm was greater than that of sandstone with thickness of 25 mm. Wu et al. [12] performed a series of mechanical tests on silty sandstone samples and found that with the increase of dry-wet cycles, the tensile strength decreased but the splitting modes were basically not influenced. Many scholars have come to a consensus that the mechanical properties of rocks are determined by the microscopic mineral structure [13–14]. Therefore, the study on the deterioration effect of sandstone strength under dry-wet cycles cannot be separated from the mesoscopic perspective. Zhang et al. [15] proposed that the multiscale physical properties, including mineral compositions, microstructures, pore size distribution characteristics, permeability and macromechanical parameters, were markedly altered during the dry-wet cycles. Yao et al. [16] conducted the Brazilian disk tests on argillaceous siltstone with dry-wet cycles, and proposed that the irreversible morphological changes in microstructures caused by the dissolution of calcite and albite were the main factor causing the decline of sandstone strength.

These studies have made some progress in the multiscale deterioration of mechanical properties of sandstone, but it is still insufficient to reveal the mechanism of mesoscopic deterioration of sandstone. In general, there are many kinds of minerals in sandstone, and complex mineral expansion/contraction and mineral dissolution occur in the process of water-rock interaction, which brings great difficulties to the study of mesoscopic mechanism [12]. Fortunately, a special sandstone, argillaceous quartz sandstone (which contains only quartz and clay minerals), was found on a bank slope in the TGRA. This special "dual structure" helps to intuitively reveal the mineral behaviors during water-rock interaction. In our previous experiments [17], we used this sandstone to reveal the possible meso-mineral evolution behaviors within rocks under the dry-wet cycles. However, it is still unclear how the tensile strength of sandstone evolves and how the mesoscopic mechanism controls the macroscopic mechanical properties. Therefore, this paper will take this sandstone as the object to carry out further dry-wet cycle test research. The Brazilian splitting tests were conducted to study the tensile strength deterioration effect, and 3D laser scanning technology was adopted to quantitatively evaluate the macroscopic failure characteristics of sandstone. In addition, the evolution characteristics of rock mesostructure were quantitatively characterized based on SEM images and fractal theory to explore the quantitative relationship between the mesostructural evolution and macro strength deterioration of sandstone. Finally, on the basis of previous theoretical studies [17], we further explored the failure process of internal minerals when sandstone was pulled apart, and how the mesostructural deterioration controlled the macro strength deterioration of sandstone.

2 Materials and methods

2.1 Specimen preparation

Specimens used in this study were collected from a bank slope of the Xietan River in the TGRA, China (Figs. 1(a) and 1(b)). The specimens were processed into cylinders with diameter and height of 50 ± 0.2 mm and 25 ± 0.2 mm, respectively (Fig. 1(c)), and the surface flatness of the specimens met the requirements of relevant specifications [18]. The X-ray diffraction results indicate that this argillaceous quartz sandstone is primarily composed of quartz (69.8%), kaolinite (16.3%), illite (12.4%), and Smectite (1.5%) [17].

2.2 Experiment instrument

The Brazilian splitting tests were carried out in the RMT-150C rock mechanics test system (Fig. 1(d)). The test system was controlled by displacement, and the loading rate was 0.02 mm/s. Tests were conducted by strictly following the relevant specifications [18].

The mesostructure of the specimens was scanned via field emission scanning electron microscopy (SEM) using a JSM-IT300HR microscope. The surface of the specimens was dusted and sprayed with gold before the tests.

The morphology features of the sandstone splitting surface were tested by a non-contact 3D topography scanner (3DScan-v4) with an accuracy of 0.001–0.05 mm.

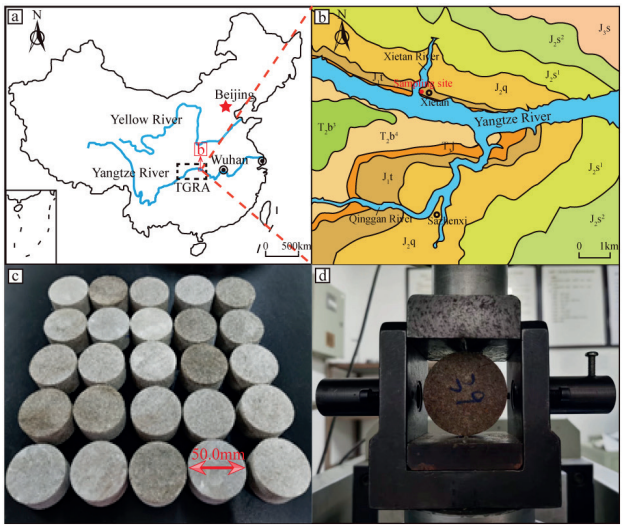

Fig. 1 Specimen sampling; (a) Location of TGRA, (b) Strata distribution in the sampling area, (c) Standard specimens, (d) Brazilian splitting test

2.3 Experiment methodology

Herein, based on the time of submersion (approximately seven months) and exposure (approximately five months) of rock mass in the hydro-fluctuation belt in the TGRA [1], 7:5 was set as the time ratio between the soaking and drying of specimens in a dry-wet cycle.

The experimental procedures were as follows: (1) The alternative sandstone specimens were dried in a 25 ℃ oven until the weight became constant. (2) Specimens that exhibited high similarity in terms of morphology, P-wave velocity, and T_2 spectrum were selected. Then, seven groups of specimens (three specimens in each group) were obtained. Among which, one group was the original group, five groups were the water-rock interaction test group, and one group was reserved as the standby group. (3) Five groups of specimens were immersed in a closed container filled with deionized water for 35 h (preliminary tests showed that specimens could reach saturation in 14 h). Afterward, the specimens were dried in a 105 ℃ oven for 25 h and then cooled to an ambient temperature (25 ℃). (4) Step 3 was repeated for 10 cycles, and one group of specimens was taken out at the end of the 1st, 3rd, 5th, 7th, and 10th cycles. (5) Finally, Brazilian splitting and SEM tests were carried out on the specimens from the water-rock interaction test group and the original group, then the fracture planes were scanned by a 3D laser.

3 Results

3.1 Strength deterioration characteristics

The tensile strength of rock can be obtained through the Brazilian splitting test, and the calculation formula is shown in Eq. (1) [11].

$$\tau = 2F / (\pi dt), \tag{1}$$

where τ is the tensile strength, F is the ultimate load when the rock specimen fails, d is the specimen diameter, and t is the specimen height.

In addition, D is the total strength deterioration rate of rock after dry-wet cycles, and $D_{i,j}$ is the average strength deterioration rate of rock after a single dry-wet cycle. The calculation formulas are shown in Eqs. (2) and (3) [19].

$$D = \left| \frac{\tau_j - \tau_0}{\tau_0} \right| \times 100\%, \tag{2}$$

$$D_{i,j} = \left| \frac{\tau_j - \tau_i}{\tau_i (j - i)} \right| \times 100\%, \tag{3}$$

where τ_0, τ_i and τ_j are the tensile strengths after the 0, i, and j dry-wet cycles, respectively.

The tensile strength and deterioration degree of rock specimens under different dry-wet cycles are shown in Table 1, and the changing trend of the tensile strength with the number of dry-wet cycles is shown in Fig. 2.

As shown in Table 1, the tensile strength of argillaceous quartz sandstone continuously deteriorated with the increase of the dry-wet cycle number, and the total strength descender of specimens under 10 dry-wet cycles reached 42.39%. In addition, the deterioration rate of sandstone strength showed a significant trend of first fast and then slow (Fig. 2). The most rapid decline in rock strength occurred at the early stage of the experiment, and the 1st dry-wet cycle resulted in a 12.44% reduction in rock strength (Table 1). Subsequently, the deterioration rate slowed down, and the average strength deterioration rate of a single dry-wet cycle was 8.41%, 6.18%, and 3.33% when the rock underwent the 1st–3rd, 3rd–5th, and 5th–7th dry-wet cycles, respectively. Finally, when the 7th–10th wet-dry cycles were performed, $D_{7,10}$ had dropped to the lowest value of 1.10%.

Table 1 Tensile strength and deterioration rate of rock specimens under different dry-wet cycles (N)

N	τ/MPa				$D_{i,j}$	D
	Spec 1	Spec 2	Spec 3	average		
0	5.81	6.19	6.34	6.11	0	0
1	5.19	5.24	5.61	5.35	12.44%	12.44%
3	4.56	4.12	4.68	4.45	8.41%	27.17%
5	4.12	3.88	3.69	3.90	6.18%	36.17%
7	3.59	3.81	3.51	3.64	3.33%	40.43%
10	3.51	3.38	3.68	3.52	1.10%	42.39%

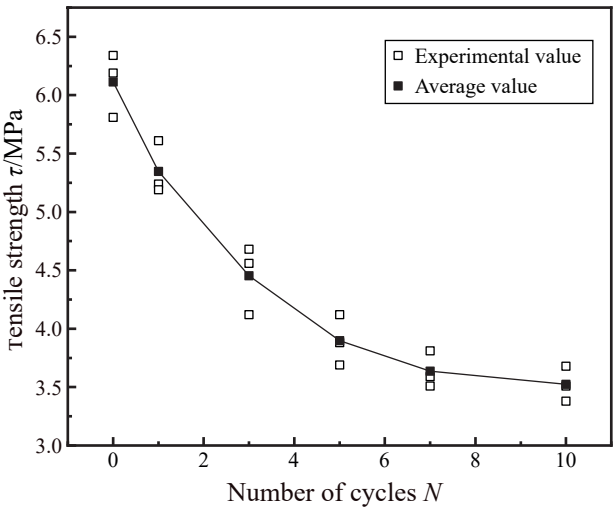

Fig. 2 Tensile strength of rock specimens under different dry-wet cycles

3.2 Morphology of fracture plane

Considering that the two fracture planes generated by the splitting test were complementary, one semicircle block of the sandstone specimen was selected for 3D scanning. After the point cloud data of all specimen fracture planes were obtained, the point coordinates in the 20 × 40 mm rectangular area in the center of the section were selected to eliminate the test error of rock debris spalling at the specimen boundary caused by water-rock interaction (Fig. 3). A coordinate system was established with disk diameter and thickness as x- and y-axes, respectively, and the vertical direction of the section as z-axis (Fig. 3) [20]. Finally, the data were processed by MATLAB to obtain the 3D morphology of each rock specimen under different dry-wet cycles (Fig. 4).

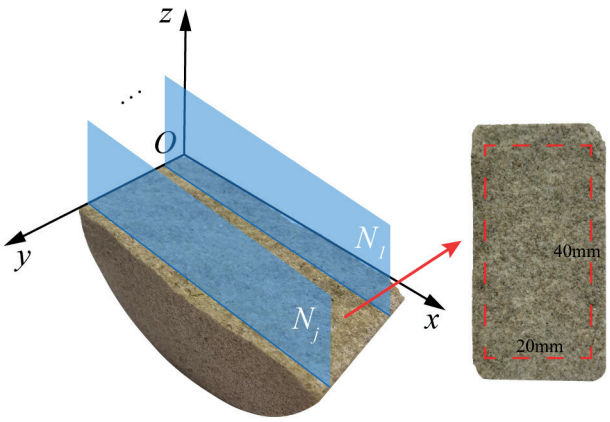

Fig. 3 Section data selection and roughness calculation method (refer to reference [20], modified)

As shown in Fig. 4, the relief (the difference between the maximum and minimum Z-values) of each sandstone specimen section was approximately 2.8–5.2 mm. Among them, the section relief of both natural rock specimens and rock specimens undergoing one dry-wet cycle was more than 5 mm, and a large area of concentrated protrusions or depressions can be observed (Figs. 4(a) and (b)). This indi-cated that the tensile fracture surface of specimens may bypass the larger particles and crystals, and break at the particle boundary with lower strength. The section relief of specimens undergoing three, five, and seven dry-wet cycles was approximately 4.2–4.5 mm. Moreover, large areas of concentrated bulges and depression remained in the sections, while the range and amplitude were slightly reduced as compared with the previous two groups of specimens, thereby suggesting a weakened obstruction degree of sandstone by particles and crystals splitting during the fracture process. Finally, after 10 dry-wet cycles, the section relief of the rock specimen was less than 3 mm, and the distribution of the protrusion and depression areas was relatively even (Fig. 4(f)), thereby indicating that the sandstone fracture surface was roughly distributed along the maximum tensile stress surface, and the rock specimen was hardly obstructed by large particles and crystals during failure.

Moreover, the root-mean-square (RMS) algorithm is one of the most popular methods to quantitatively evaluate structural surface roughness [21]. Meanwhile, the intuitionistic and clear description of section relief in the previous article has made up for the shortcoming of the RMS method in considering the maximum amplitude. Therefore, the RMS method is used to further quantitatively evaluate the influence of dry-wet cycles on the section roughness.

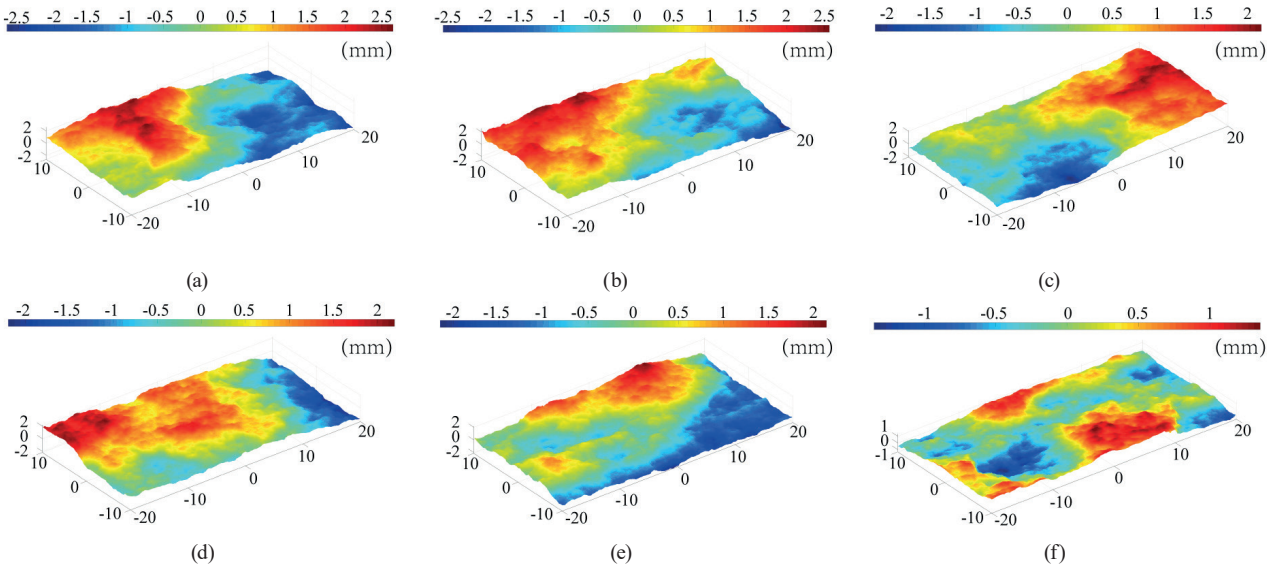

Fig. 4 Morphologies of sandstone sections under different dry-wet cycles; (a) $N = 0$, (b) $N = 1$, (c) $N = 3$, (d) $N = 5$, (e) $N = 7$, (a) $N = 0$, (f) $N = 10$

Suppose there are m planes parallel to the plane XOZ, and the intersection lines with the plane XOY are shown in Fig. 3. Then, the evaluation index of the specimen section roughness C_{JR} can be calculated as follows [22]:

$$C_{JR} = 51.85\left(Z_2\right)^{0.60} - 10.37, \tag{4}$$

$$Z_2 = \left[\frac{1}{mH}\sum_{i=1}^{n}\sum_{j=1}^{m}\frac{\left(z_{ij} - z_{ij-1}\right)^2}{x_{ij} - x_{ij-1}}\right]^{\frac{1}{2}}, \tag{5}$$

where Z_2 is the RMS slope, H is the effective length of the intersection line in the x direction, and n is the number of equidistant points chosen at the intersection line.

Based on the changes in the C_{JR} value (Fig. 5), the roughness of sandstone sections generally showed a decreasing trend as the number of dry-wet cycles increased, and the total decrease after 10 dry-wet cycles was 8.5%. During the experiment, the first dry-wet cycle caused the largest reduction of sandstone section roughness, which was 2.9%. In addition, the roughness of specimens undergoing five wet-dry cycles was slightly greater than that of specimens undergoing three wet-dry cycles, which may be due to the individual dispersion of the specimens and the contingency of the tests. Combined with Figs. 4 and 5, it can be concluded that with the increase of dry-wet cycles, both the relief and roughness indexes of the sandstone fracture section generally showed a downward trend.

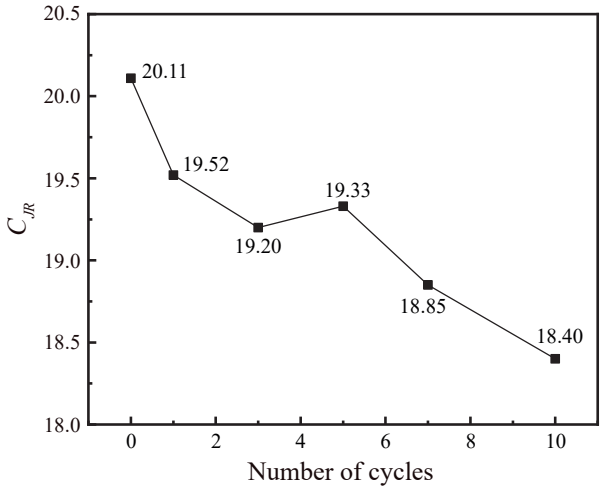

Fig. 5 value of C_{JR} under different dry-wet cycles

3.3 Fractal dimension characterization based on SEM

The fractal theory can be applied to quantitatively evaluate the observed mesoscopic defects (such as pores and cracks) in rocks. The commonly used methods include Hausdorff dimension method, variational dimension method, box dimension method, and so on [23–25], among which, the box dimension method is the most suitable to describe the pores and cracks in the rock.

Firstly, SEM images of sandstone were processed into binary digital images by setting appropriate gray thresholds (Fig. 6). The calculation process of fractal box dimension was as follows: (1) The image was continuously segmented by square boxes with side length δ, and the number of boxes covering pores and cracks was recorded as $N(\delta)$. (2) The side length δ was continuously reduced to 0, and it was drawn together with the corresponding $N(\delta)$ into the double logarithmic coordinate plane, then the fractal dimension d can be obtained by linear fitting as follows:

$$d = -\lim_{\delta \to 0}\frac{\lg N\left(\delta\right)}{\lg \delta}. \tag{6}$$

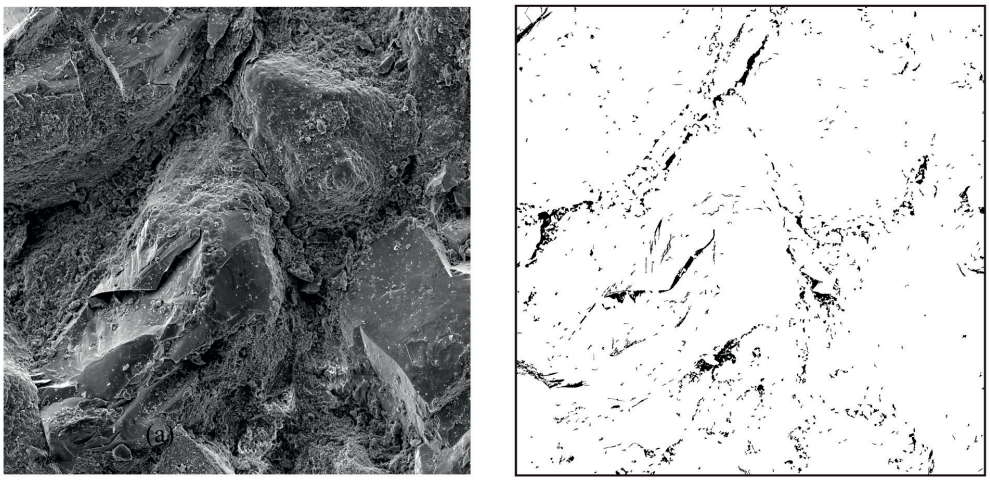

(a) (b)

Fig. 6 Binary processing of sandstone SEM images; (a) The original SEM image, (b) The binary image of SEM

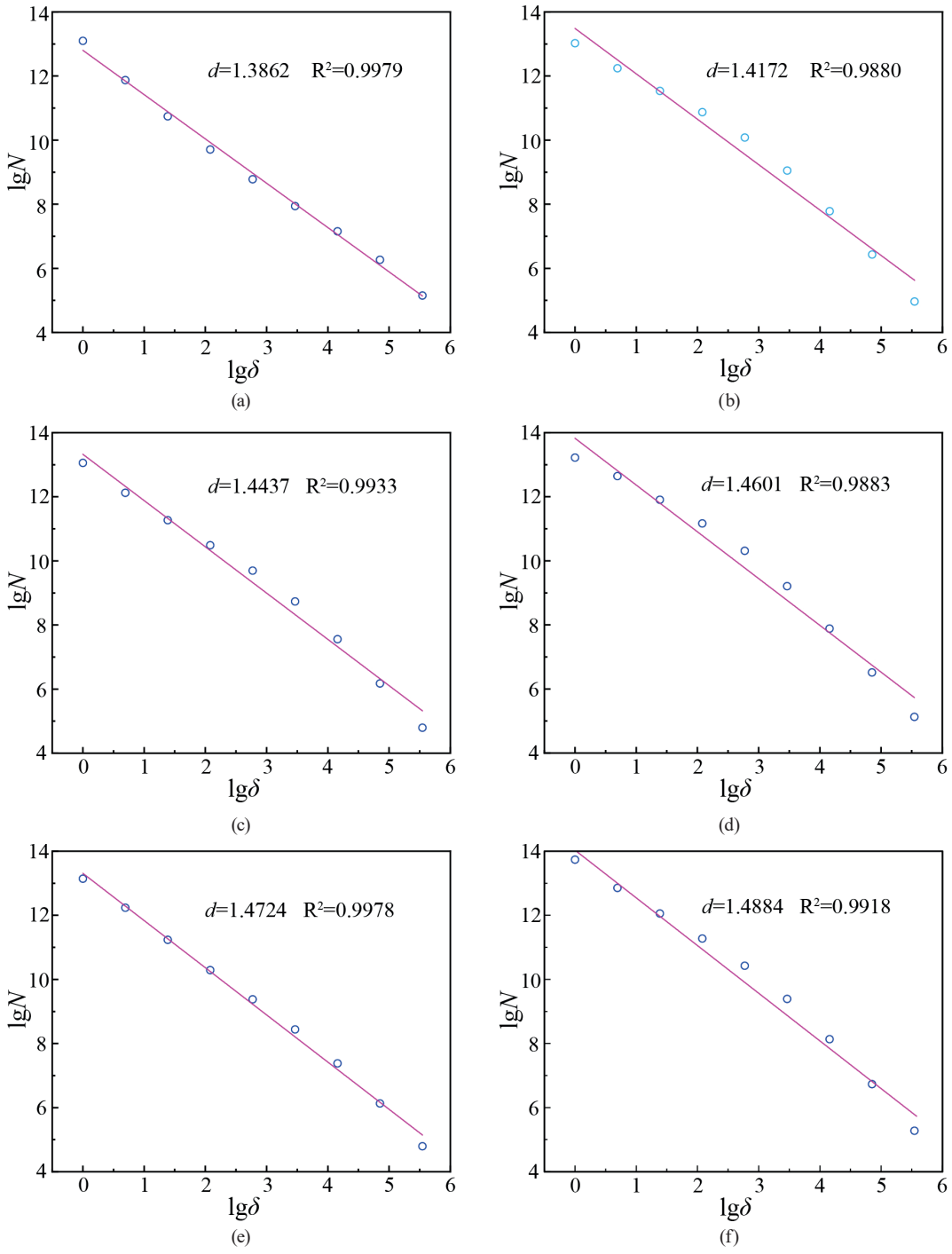

Fig. 7 Fractal dimension of sandstone under different dry-wet cycles
(a) N = 0, (b) N = 1, (c) N = 3, (d) N = 5, (e) N = 7, (f) N = 10

The SEM images (×200 times) of sandstones undergoing 0, 1, 3, 5, 7, and 10 dry-wet cycles were treated above, and the fractal dimension of sandstone mesostructure under different dry-wet cycles was shown in Fig. 7.

As shown in Fig. 7, each correlation coefficient R^2 was greater than 0.988, thereby suggesting that the distribution of pores and cracks in sandstone had good fractal characteristics, and the fitting results were highly reliable. During the 0–10 dry-wet cycles, the fractal dimension of the sandstone continuously increased, thereby indicating that the pores and cracks in the sandstone continued to develop and expand. Thus, their distribution was increasingly complex, and the integrity of the sandstone mesostructure became worse.

4 Discussion

4.1 Multi-parameter characterization of tensile strength

Sandstone is a typical porous medium, and its internal pores and cracks are the structural "defects" that adversely affect its strength. The porosities of sandstone under different dry-wet cycles (N) have been measured by NMR (Table 2) [17]. Herein, porosity and fractal dimension are the mesoscopic parameters based on 3D or 2D scales, respectively, to characterize the distribution of pores and cracks in sandstone. As shown in Table 2 and Fig. 7, with the increase of dry-wet cycles, the porosity and fractal dimension of the sandstone kept rising, thereby indicating that the pores and cracks in the sandstone continued to develop. This phenomenon revealed that the sandstone mesostructure suffered deterioration, which also reflected the deterioration of the macroscopic tensile strength (Table 1). The evolution laws of porosity, fractal dimension, and deterioration rate of strength along with the dry-wet cycles (N) were shown in Fig. 8.

As shown in Fig. 8, porosity, fractal dimension, and deterioration rate of strength were positively correlated with the number of dry-wet cycles, and the evolution relationship conformed to the exponential function as follows:

$$y = A\exp\left(N/t\right) + B \tag{7}$$

where A, t, and B were fitting parameters, and N was the number of dry-wet cycles.

The correlation coefficients of the D, n, and d with the N were all greater than 0.99, which proved reliable fitting results. Moreover, the fitting curve shapes of the three were highly similar, thereby indicating that porosity and fractal dimension had a marked impact on the deterioration rate of sandstone tensile strength, that is, the deterioration of sandstone mesostructural parameters can well characterize the macroscopic strength deterioration characteristics. Therefore, the relationship between porosity, fractal dimension, and tensile strength can be further obtained (Fig. 9).

Table 2 Sandstone porosity under different dry-wet cycles

N	0	1	3	5	7	10
porosity n/%	3.73	4.19	4.85	5.35	5.70	5.87

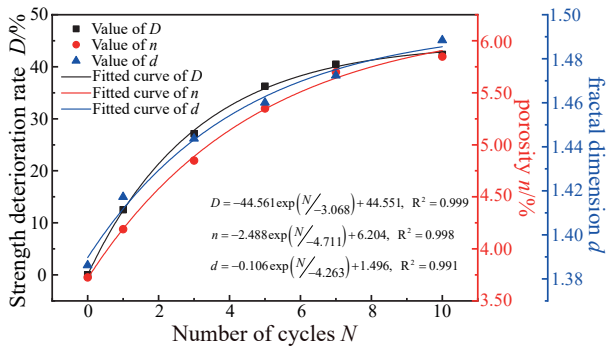

Fig. 8 The relationship between porosity, fractal dimension, and deterioration rate of strength and the number of dry-wet cycles

4.2 Evolution process of sandstone strength deterioration

Through our previous research, it has been concluded that the mesostructural deterioration mechanism and mineral evolution rule of argillaceous quartz sandstone under dry-wet cycles [17]: repeated "absorption and swelling-dehydration and contraction" of clay minerals leads to the repeated physical action of "loading-unloading" process in sandstone, thereby resulting in the breakage of framework mineral quartz (Fig. 10). Therefore, on this basis, this study will further discuss how the mesoscopic mineral behaviors control the deterioration of sandstone tensile strength.

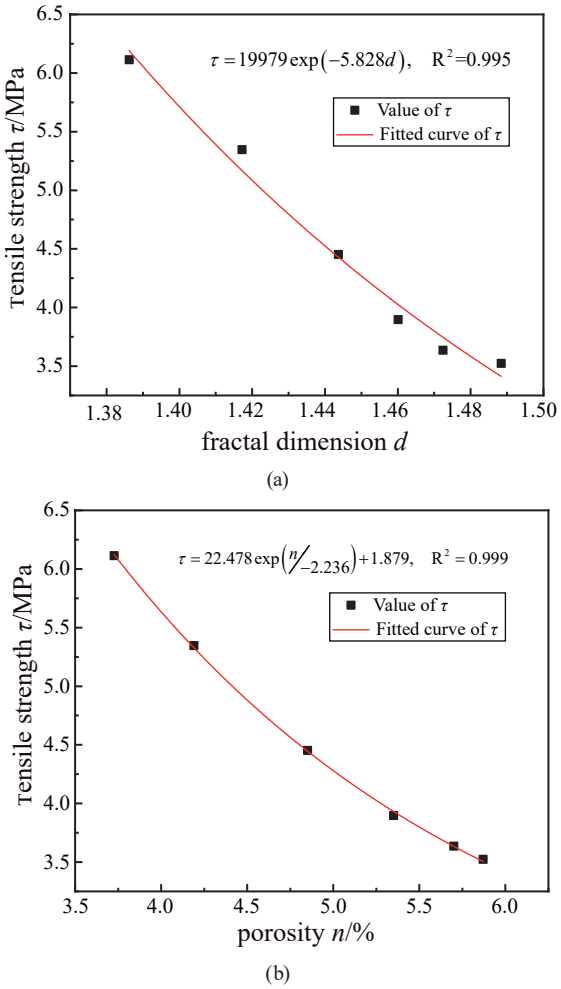

Fig. 9 Relationship between tensile strength and mesoscopic parameters; (a) Fitted curve of the τ and the d, (b) Fitted curve of the τ and the n

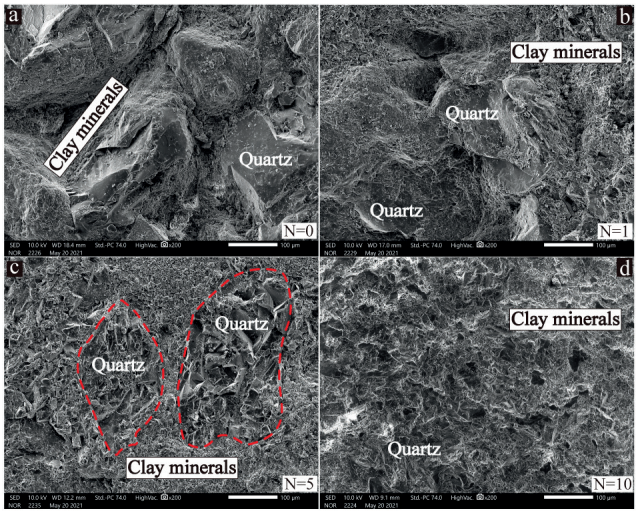

Fig. 10 SEM images of sandstone under different dry-wet cycles (×200 times) (cited in literature [17])

During the Brazilian splitting test, the maximum tensile stress was distributed along the diameter of the parallel loading direction, hence, the sandstone tensile strength depended on the difficulty of breaking the minerals on this diameter. In this study, sandstone was pore-cementation, and clay minerals were filled around quartz as filling materials. Clay minerals with loose structure and low strength will be pulled apart before quartz during loading, then the sandstone tensile strength will be primarily borne by quartz particles. The complete quartz particles were strong and cannot be easily broken directly, hence, the final tensile surface may present the following two forms [26]: (1) When passing through the unbroken quartz particles, cracks will expand along the weak part of the quartz boundary; and (2) when passing through the broken quartz grains, the cracks will pass directly through the quartz interior. When the quartz in the sandstone was relatively complete, the tensile strength of the sandstone will be significantly greater than that of the sandstone with relatively broken quartz particles. Thus, a schematic diagram of the Brazilian splitting test process was drawn (Fig. 11) to reveal the influence of dry-wet cycles more intuitively on the mineral morphology evolution and tensile strength of sandstone, then it was discussed and verified combined with the fracture section morphology (Figs. 4 and 5).

Without the dry-wet cycling, the overall structure of quartz particles in the original sandstone was relatively complete (Figs. 10(a) and 11(a)), and the distribution of internal cracks was less, which was reflected in the low fractal dimension (Fig. 7). During loading, quartz particles were strong and cannot be easily broken, hence the sandstone tensile strength was relatively high (Fig. 11 (b)). Precisely because the complete quartz particles were difficult to be pulled apart by the transverse tension, the section may bypass the quartz and split at the grain boundary, thereby resulting in a large number and amplitude of protrusions and depressions on the fault surface (Fig. 11 (c)). At this time, high values were shown in both the relief and roughness of the split section.

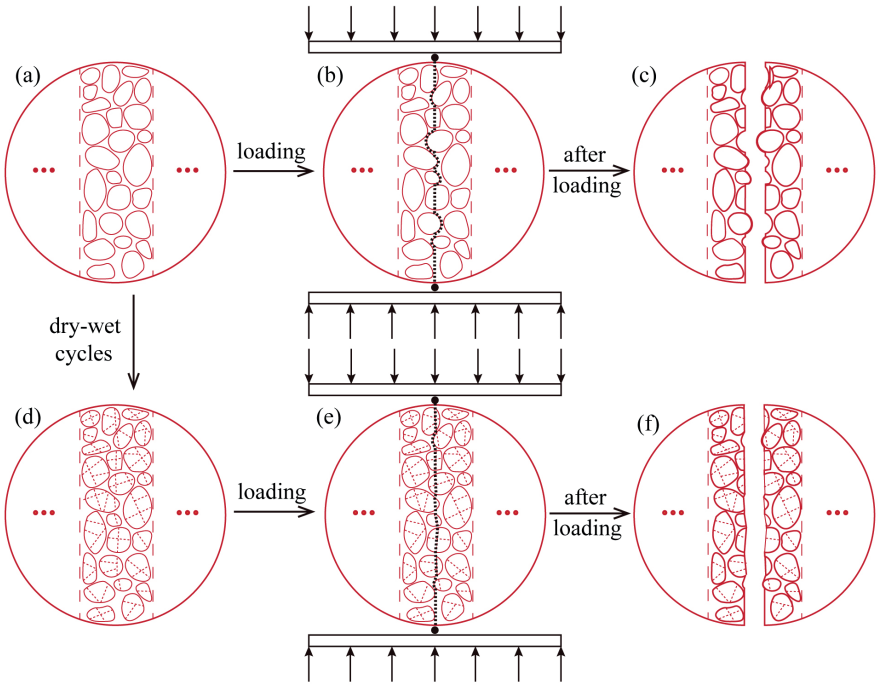

Fig. 11 Schematic diagram of splitting failure evolution of sandstone under different dry-wet cycles; (a) Original sandstone, (b) Sandstone during loading, (c) Sandstone after loading, (d) Sandstone after dry-wet cycles, (e) Sandstone (after dry-wet cycles) during loading, (f) Sandstone (after dry-wet cycles) after loading

After several dry-wet cycles of sandstone, quartz particles were constantly broken (Fig. 10), thereby showing the phenomenon of "from large to small" (Figs. 10(d) and 11(d)). Numerous cracks appeared in quartz, the framework mineral bearing the main strength of rocks, and the fractal dimension increased. At this time, when the splitting test was carried out, cracks could be connected from the inside of large quartz particles that were previously difficult to be pulled apart (Fig. 11(e)), thereby resulting in greater deterioration of sandstone tensile strength. Furthermore, with the increase of dry-wet cycles, the large-grained quartz became increasingly broken, and the number of quartz particles that needed to be bypassed by the splitting section decreased continuously. Consequently, the amplitude of protrusions and depressions on the fault surface was smaller and their distribution became more uniform (Fig. 11(f)), which was reflected in the numerical values that the relief and roughness of the section were continuously reduced as compared with the original sandstone (Figs. 4 and 5).

Based on the above analysis, the dry-wet cycles primarily caused the repeated "expansion-contraction" of clay minerals, and finally made the mesoscopic structure of sandstone appear as the framework mineral quartz particles constantly broken. In this study, the continuous development and connection of internal cracks in sandstone led to marked deterioration of mesostructured, which was the main controlling factor for the deterioration of sandstone strength and the reduction of splitting section roughness.

5 Conclusions

1. Dry-wet cycles lead to marked deterioration of sandstone tensile strength characterized by a rapid decline at first and then a gradual flattening. The relief and roughness of the sandstone splitting section also generally show a decreasing trend with dry-wet cycles.
2. With the increase of dry-wet cycles, the fractal dimension and porosity of sandstone continue to rise, thereby indicating that the sandstone mesostructure suffers from deterioration. Moreover, the change rules of the two are highly consistent with that of the tensile strength, thereby proving that the deterioration of the mesoscopic parameters can well characterize the deterioration effect of the macroscopic tensile strength. Finally, the mathematical relationship between the tensile strength of sandstone and the above two is established.
3. After the dry-wet cycles, the clay minerals repeatedly "expand and contract" and constantly squeeze the quartz, thereby resulting in numerous cracks in the particles. When loading, the splitting surface will pass through the cracks in the quartz particle rather than bypass the grain boundary, hence, quartz particles can be easily pulled apart and the tensile strength of the sandstone is reduced.

Acknowledgement

This work was supported by Special Research Funds for National Field Observation and Research Station of Landslides in Three Gorges Reservoir Area of Yangtze River (Ministry of Science and Technology) (Z2022106), and Special Research for the Deterioration of Rock Mass of Bank Slopes in Three Gorges Reservoir Area of Yangtze River in Hubei Province. (HZ2021120). Thoughtful reviews and the comments of editors and anonymous reviewers helped us to strengthen the manuscript.

References

[1] Tang, H., Wasowski, J., Juang, C. H. "Geohazards in the three Gorges Reservoir Area, China – Lessons learned from decades of research", Engineering Geology, 261, 105267, 2019. https://doi.org/10.1016/j.enggeo.2019.105267

[2] Yin, Y., Huang, B., Zhang, Q., Yan, G., Dai, Z. "Research on recently occurred reservoir-induced Kamenziwan rockslide in Three Gorges Reservoir, China", Landslides, 17, pp. 1935–1949, 2020. https://doi.org/10.1007/s10346-020-01394-7

[3] Sun, Q., Zhang, Y. "Combined effects of salt, cyclic wetting and drying cycles on the physical and mechanical properties of sandstone", Engineering Geology, 248, pp. 70–79, 2019. https://doi.org/10.1016/j.enggeo.2018.11.009

[4] Ying, P., Zhu, Z., Ren, L., Deng, S., Niu, C., Wan, D., Wang, F. "Deterioration of dynamic fracture characteristics, tensile strength and elastic modulus of tight sandstone under dry-wet cycles", Theoretical and Applied Fracture Mechanics, 109, 102698, 2020. https://doi.org/10.1016/j.tafmec.2020.102698

[5] Du, B., Cheng, Q., Miao, L., Wang, J., Bai, H. "Experimental study on influence of wetting-drying cycle on dynamic fracture and energy dissipation of red-sandstone", Journal of Building Engineering, 44, 102619, 2021. https://doi.org/10.1016/j.jobe.2021.102619

[6] Bagde, M. N., Petros, V. "Fatigue properties of intact sandstone samples subjected to dynamic uniaxial cyclical loading", International Journal of Rock Mechanics and Mining Sciences, 42(2), pp. 237–250, 2005. https://doi.org/10.1016/j.ijrmms.2004.08.008

[7] Xu, Z.-H., Feng, G.-L., Sun, Q.-C., Zhang, G.-D., He, Y.-M. "A modified model for predicting the strength of drying-wetting cycled sandstone based on the P-Wave velocity", Sustainability, 12(14), 5655, 2020.
https://doi.org/10.3390/su12145655

[8] Luo, Z., Li, J., Jiang, Q., Zhang, Y., Huang, Y., Assefa, E., Deng, H. "Effect of the Water-Rock Interaction on the Creep Mechanical Properties of the Sandstone Rock", Periodica Polytechnica Civil Engineering, 62(2), pp. 451–461, 2018.
https://doi.org/10.3311/PPci.11788

[9] Zhao, B., Li, Y., Huang, W., Yang, J., Sun, J., Li, W., Zhang, L., Zhang, L. "Mechanical characteristics of red sandstone under cyclic wetting and drying", Environmental Earth Sciences, 80, 738, 2021.
https://doi.org/10.1007/s12665-021-10067-0

[10] Yao, W., Li, C., Zhan, H., Zhou, J., Criss, R., Xiong, S., Jiang, X. "Multiscale study of physical and mechanical properties of sandstone in Three Gorges Reservoir Region subjected to cyclic wetting-drying of Yangtze River water", Rock Mechanics and Rock Engineering, 53, pp. 2215–2231, 2020.
https://doi.org/10.1007/s00603-019-02037-7

[11] Liu, X., Wang, Z., Fu, Y., Yuan, W., Miao, L. "Macro/microtesting and damage and degradation of sandstones under dry-wet cycles", Advances in Materials Science and Engineering, 2016, 7013032, 2016.
https://doi.org/10.1155/2016/7013032

[12] Wu, Q., Liu, Y., Tang, H., Kang, J., Wang, L., Li, C., Wang, D., Liu, Z. "Experimental study of the influence of wetting and drying cycles on the strength of intact rock samples from a red stratum in the Three Gorges Reservoir area", Engineering Geology, 314, 107013, 2023.
https://doi.org/10.1016/j.enggeo.2023.107013

[13] Wang, C., Pei, W., Zhang, M., Lai, Y., Dai, J. "Multi-scale experimental investigations on the deterioration mechanism of sandstone under wetting–drying cycles", Rock Mechanics and Rock Engineering, 54, pp. 429–441, 2021.
https://doi.org/10.1007/s00603-020-02257-2

[14] Zhang, H., Lu, K., Zhang, W., Li, D., Yang, G. "Quantification and acoustic emission characteristics of sandstone damage evolution under dry–wet cycles", Journal of Building Engineering, 48, 103996, 2022.
https://doi.org/10.1016/j.jobe.2022.103996

[15] Zhang, C., Dai, Z., Tan, W., Yang, Y., Zhang, L. "Multiscale study of the deterioration of sandstone in the Three Gorges Reservoir Area subjected to cyclic wetting–cooling and drying–heating", Rock Mechanics and Rock Engineering, 55, pp. 5619–5637, 2022.
https://doi.org/10.1007/s00603-022-02929-1

[16] Yao, W., Li, C., Ke, Q., Fan, Y., Li, B., Zhan, H., Criss, R. "Multiscale deterioration of physical and mechanical properties of argillaceous siltstone under cyclic wetting-drying of Yangtze River water", Engineering Geology, 312, 106925, 2023.
https://doi.org/10.1016/j.enggeo.2022.106925

[17] Deng, L., Yang, J., Zhang, G., Zhang, Y., Chen, G., Li, X. "Damage Characteristics of Argillaceous Quartz Sandstone Mesostructure under Different Wetting-drying Conditions", Periodica Polytechnica Civil Engineering, 66(3), pp. 785–797, 2022.
https://doi.org/10.3311/PPci.19662

[18] Fairhurst, C. E., Hudson, J. A. "Draft ISRM suggested method for the complete stress-strain curve for intact rock in uniaxial compression", International Journal of Rock Mechanics & Mining Science, 36(3), pp. 281–289, 1999.
https://doi.org/10.1016/S0148-9062(99)00006-6

[19] Liu, X., Yuan, W., Fu, Y., Wang, Z., Miao, L., Xie, W. "Porosity evolution of sandstone dissolution under wetting and drying cycles", Chinese Journal of Geotechnical Engineering, 40(3), pp. 527–532, 2018. (in Chinese)
https://doi.org/10.11779/CJGE201803017

[20] Han, Y., Wang, Z., Tang, Y. "Mechanical behavior of different rocks in the splitting test", Journal of China University of Mining and Technology, 49(5), pp. 863–873, 2020. (in Chinese)
https://doi.org/10.13247/j.cnki.jcumt.001192

[21] Zhang, G., Karakus, M., Tang, H., Ge, Y., Zhang, L. "A new method estimating the 2D Joint Roughness Coefficient for discontinuity surfaces in rock masses", International Journal of Rock Mechanics and Mining Sciences, 72, pp. 191–198, 2014.
https://doi.org/10.1016/j.ijrmms.2014.09.009

[22] Tatone, B. S. A., Grasselli, G. "A new 2D discontinuity roughness parameter and its correlation with JRC", International Journal of Rock Mechanics and Mining Sciences, 47(8), pp. 1391–1400, 2010.
https://doi.org/10.1016/j.ijrmms.2010.06.006

[23] Hirose, K., Matsubara, H. "Mechanisms of mudcrack formation and growth in bentonite paste", Journal of Geotechnical and Geoenvironmental Engineering, 144(4), 04018017, 2018.
https://doi.org/10.1061/(ASCE)GT.1943-5606.0001853

[24] Berizzi, F., Bertini, G., Martorella, M., Bertacca, M. "Two-dimensional variation algorithm for fractal analysis of sea SAR images", IEEE Transactions on Geoscience and Remote Sensing, 44(9), pp. 2361–2373, 2006.
https://doi.org/10.1109/TGRS.2006.873577

[25] Wu, M., Wang, W., Shi, D., Song, Z., Li, M., Luo, Y. "Improved box-counting methods to directly estimate the fractal dimension of a rough surface", Measurement, 177, 109303, 2021.
https://doi.org/10.1016/j.measurement.2021.109303

[26] Zhu. C., Li, W., An, Y., Wang, Y. "Crack propagation process of transparent rock-like material under Brazilian splitting", Chinese Science and Technology Papers, 17(7), pp. 764–769, 2022. (in Chinese)
https://doi.org/10.3969/j.issn.2095-2783.2022.07.010